



Iranian Research Organization
for Science and Technology
(IROST)

Advances
Environmental
Technology



Journal home page: <https://aet.irost.ir/>

Stirred tank reactor with dual impeller Rushton turbine for application of wastewater treatment - Process optimization and CFD simulation

Shivanand M Teli, Sunil J Kulkarni*

Chemical Engineering Department, GF's Gharda Institute of Technology, Khed, India

ARTICLE INFO

Document Type:

Research Paper

Article history:

Received 1 May 2023

Received in revised form

17 August 2023

Accepted 18 August 2023

Keywords:

Biological treatment

Optimization

Small scale industrial
wastewater

Coefficient

Configurations

hydrodynamics

Fluid dynamics

ABSTRACT

The treatment of industrial wastewater by economical and efficient methods is being explored to improve treatment efficiency and costs. Wastewater treatment via biological methods to reduce carbonaceous matter is common in the form of an activated sludge process (ASP). In the current work, the aerobic decomposition of waste was carried out in a reactor with constant stirring with a Rushton type turbine. The optimum values of the flow rate of air were obtained for two reactor impeller configurations for better waste degradation. The extent of degradation in the stirred tank reactor was studied for different values of impeller clearances. Two configurations, C1 and C2, were investigated. It was observed that under a continuous air supply for 36 hours, the impeller configuration C2 provided 80% degradation compared to 74.4 % for C1. Increased values of superficial gas velocity (U_G) and impeller speed resulted in decreased degradation due to shear stress on microorganisms for two impeller configurations. The hydrodynamic study confirmed that the impeller configuration C1 required less power consumption than C2 for the same operating condition. The k-epsilon turbulent model and the population balance model were used in combination. The models were validated with the experimental results of the hydrodynamic parameters for the values of operating parameters over a considerable range. The forecasting of mass transfer coefficients from different models was compared with practically determined values for the two configurations of impeller positions in the tank.

1. Introduction

The sources of wastewater can be industrial, domestic, commercial, agricultural, horticultural, seawater, pond water, any sewer inflow or sewer infiltration, and aquaculture effluent. The

treatment of domestic and industrial waste is putting limitations on the advantages of industrial growth. The industrial revolution is an unavoidable and progressive phenomenon. The other side of the industrial revolution is the environmental and

*Corresponding author Tel.: +91 96658 16241

E-mail: suniljayantkulkarni@gmail.com

DOI:10.22104/AET.2023.6207.1710

COPYRIGHTS: ©2023 Advances in Environmental Technology (AET). This article is an open access article distributed under the terms and conditions of the Creative Commons Attribution 4.0 International (CC BY 4.0) (<https://creativecommons.org/licenses/by/4.0/>)

ecological imbalance due to the footprints of industrialization. The treatment of liquid effluent is very important from a health perspective. Liquid effluent needs to be treated to remove organic and inorganic pollutants. Stabilizing the organic content and converting it into settleable material is one way to deal with these pollutants. Presently, the major methods engaged for industrial wastewater treatment are based on physico-chemical principles [1]. Physical and chemical wastewater treatment methods have drawbacks, including high cost, ineffectiveness, and chemical contamination. For toxic waste, biological treatments are economical and safe. Bioremediation for treating toxic waste is one of the most practiced methods for treating these wastes. Biological treatments can be in the presence or absence of air. Biological treatment supported by aerobic and anaerobic biological methods employs microorganisms for the degradation of organic matter. The unstable organic waste gets oxidized under aerobic and anaerobic conditions. Aerobic treatment degrades/oxidizes organic impurities. Breaking organic impurities without oxygen produces methane, carbon dioxide, and other biomass in anaerobic treatment. Gas liquid mass transfer can be improved by using various methods and modifying the equipment. Proper distribution of air is a very important aspect in this context. Types of aerators include diffused, mechanical, and gravity aerators that are used for industrial wastewater treatment. One of the important suspended growth methods is the activated sludge process [2]. Hydrogen sulphide (H_2S) can be removed from wastewater by diffused air in the ASP [3]. In ASP, an aerobic mechanism for biodegrading and nitrifying waste calls for a high oxygen transfer rate. Aeration effect studies in ASP are reported in the literature [4]. Oxygen utilization can be made more effective using fine bubble aeration with a compressed gas system. Various utilities can be employed for consistent operation and betterment in efficiency and conversion. Understanding the bioreactors' response is significant in inducing higher wastewater treatment plant efficiency. The wastewater treatment in stirred tank reactors has been widely studied in the past three decades [5-10]. Biogas manufacturing using wheat and pearl

millet straw and corn stalk under anaerobic digestion in a CSTR has been reported in the literature [11,12]. Batch reactors are popular due to their operational flexibility and ease of controlling process parameters. The effect of several stages and bioreactor types has been reported in the literature [13]. The biological activated charcoal treatment of commercial-scale wastewater in a stirred tank reactor has been reported by an investigator [6]. Aerobic stirred tank reactors can be combined with adsorption by adding biological adsorbent (carbon). Reactors with a cavitation facility can be used for AOP (advanced oxidation) [1,14,15]. The photovoltaic and photochemical pathways, photocatalysis, and physical and chemical treatments are restricted due to costs and limitations in the application. Effluent processing by these methods needs chemicals, precursors, and energy. Due to energy costs and carbon dispersion, scientists are exploring safe, calm, and smooth treatments for wastewater. Wastewater treatment on a large scale is a challenging task with advanced separation techniques. Computational fluids dynamic (CFD) is one of the most effective and sought-after tools for design. CFD is an advantageous modelling tool in the industry because of its excellent visualization technique that allows studies of the characteristics of fluid flow in detail and visualization of the local-scale phenomena in varying operating conditions. The CFD tool is used for economic optimization and retrofitting of existing treatment plants. The first model of CFD for the optimization of ASP was demonstrated for reliable transport and settling by Randal and Wicklein [16]. CFD has become the most sought-after tool for designing and scaling multiphase reactors. The process design and analysis of different unit operations are essential in designing and optimizing an effluent treatment plant. The treatment tank can be visualized using the complete transport modeling approach [17-20]. CFD modeling is engaged for the gas-liquid contact in effluent treatment reported in the literature [21]. Acceptance of CFD by experts has been on the rise because of its applicability. The stirred tanks as bioreactors are popular because of their design flexibility and good transfer characteristics (mass and heat) [22]. The shear stress offered is significant for biological

wastewater treatment processes. The stirred tank reactor is suitable for several biological reactions involving shear-sensitive cells. Considering installation and operating expenses, stirred tank reactors with advanced tools are economical for large-scale treatments and need to be optimized for small-scale industries. In the present work, tank reactors with stirring were used for the treatment of effluent from agrochemical industries. The microorganism culture was provided by nearby industries. The CFD simulation was performed using a k-epsilon turbulent model with bubble break-up, and a coalescence mechanism was applied with simulations. The impeller configurations were studied for the effect on the hold-up of gas and distribution of droplet size; the coefficient of mass transfer in the tank reactor was determined from the experimental and CFD simulation predictions. The comparison of different mass transfer models, namely the penetration model, slip velocity model, rigid cell model, and eddy cell model for different impeller speeds of 120 to 270 rpm for fixed superficial gas velocity, was carried out. The investigation aims to evaluate the feasibility of a stirred tank reactor with a dual impeller Rushton turbine for the aerobic digestion of industrial effluent to provide better biological organisms cultivation and treat wastewater. The objective of the current work was the utilization of a biological treatment method for wastewater treatment and coupling this conventional treatment with a modern approach. Many investigations have been reported on biological treatments with advanced applications, namely advanced oxidation processes, ultraviolet light mediated treatments, and cavitation based biological treatments. The optimization of contacting equipment, like the stirred tank reactor with specific applications for wastewater treatment, is not a much-explored area of investigation. Also, a modern computational tool was used for studying the flow patterns and interrelations between various parameters.

2. Materials and methods

2.1. Wastewater and other reagents

Reagents required for the determination of COD were obtained from a distributor from Mumbai, India. The Lote Parshuram industrial area near Khed is the hotspot of chemical industries. Many agrochemicals, bulk, and fine chemical manufacturers have located their plants in this vicinity. The Maharashtra Industrial Development and Corporation (MIDC) is a government agency formed by the Maharashtra government to provide facilities and support to industrialists. The effluent and sludge were brought from the agro-industry located in MIDC, near Chiplun, Maharashtra. The samples were stored at 4 °C. The COD and BOD of samples were 4346 mg/l and 3000 mg/l, respectively. The suspended solids and total solids were 800 mg/l and 3260 mg/l, respectively, whereas the total organic carbon was 1965 to 2190 mg/l.

2.2. Experimental setup

The set up required for experimentation was prepared at the Department of Chemical Engineering, mass transfer operation laboratory at the Gharda Foundations College of Engineering located near the industrial zone of Lote Parshuram near Khed in Maharashtra, India. A dual impeller stirred tank reactor was employed for treating the effluent. The dimensions of the stirred tank reactor are tabulated in Table 1. The schematic diagram of the stirred tank reactor with a dual impeller Rushton turbine is shown in Figure 1. The experiments were conducted at prevailing laboratory conditions (28 °C). The semi-batch mode was used. In this, the air was supplied to the reactor in a continuous way. Then, wastewater and biomass (sludge) were introduced into the reactor. The operating parameters, like flow rate of air, speed of agitation, impeller, wastewater flow rate, and sludge loading in a reactor, are given in the following section.

Table 1. Geometrical dimensions of stirred tank reactor with dual impeller Rushton turbine.

Dimension	Value	Units
Inner tank diameter (T)	0.30	m
The ratio of height to diameter of tank	H/T = 2	(-)
Impeller to Tank diameter (T)	D/T = 1/3	(-)
The total volume of the reactor	0.042	m ³
Fixed bottom impeller location	h/T = 0.55	(-)
Upper impeller location For C1 case	h/T = 0.86	(-)
Upper impeller location For C2 case	h/T = 1.2	(-)
Number of holes on ring sparger	32	No
Ring sparger diameter	0.15	m

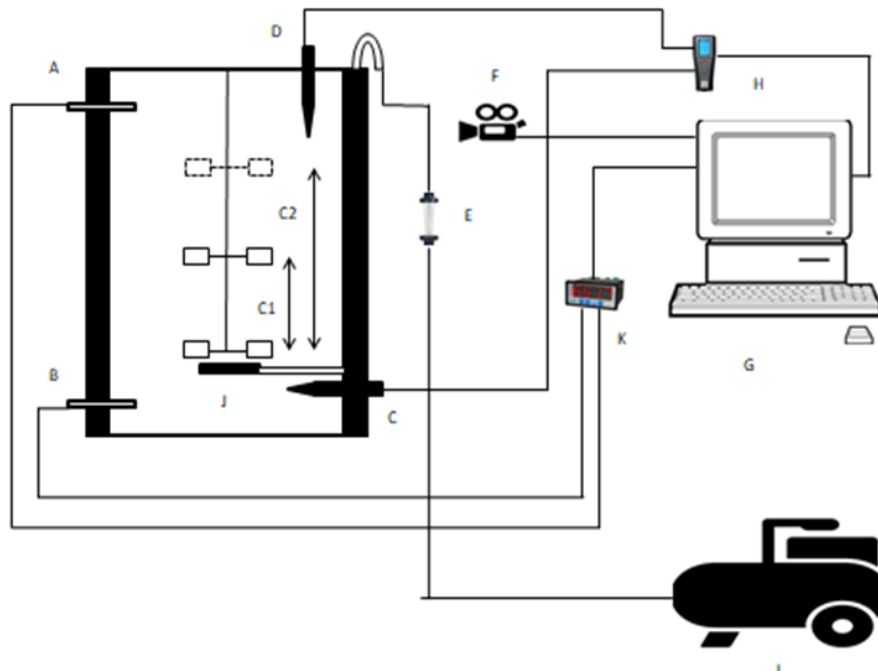


Fig. 1. Schematic diagram of stirred tank reactor with Rushton, turbine, A & B Pressure sensor, C & D Dissolved oxygen probe, E Flow meter, F Camera, G Computer, H Dissolved oxygen meter with data acquisition meter, I Double acting compressor, J Ring Sparger 24 holes, 2 mm size, K Pressure measure with data acquisition meter.

2.3. Experimental Procedure

2.3.1. Stirred tank reactor with dual impeller Rushton turbine.

The method used for the COD determination of the wastewater is discussed in section 2.4. For consistent quality, the wastewater was used after dilution. For every run, 25 litres of water, 10 litres of liquid waste, and 3 litres of solid biological mass were required. The volume of wastewater and biomass culture together was 38 litres. The air was supplied at a particular superficial gas velocity range (0.828 m/h to 5.76 m/h) equal to that used in aeration for the growth of microbes. The superficial gas velocity was again optimized for the

system. COD was determined after every four hours, and this was continued for 40 hours. Then, the airflow rate and impeller speed were varied. The impeller was fitted at $h/T = 0.55$, while the upper impeller was adjusted at various locations relative to the bottom impeller. For the C1 case, the upper impeller was located at $h/T = 0.8$, and for the C2 case, at $h/T = 1.2$. A reduction in COD was observed for both C1 and C2 configurations. The degradation % of wastewater was determined for the dual impeller configuration and then compared. The experiments were carried out to determine the important parameters that have a significant effect on the transport processes. The physical property of water was considered during the

experiment & CFD simulation. Water and air were used in the continuous and disperse phase, respectively. Detailed experimentation and adopted methods at different stages of the investigations are elaborated in section 3.

2.4. Chemical oxygen demand (COD)

The oxygen demand is determined by using an oxidising agent at 80°C for two and a half hours. If the wastewater contains an oxygen deficit, it can reduce the dissolved oxygen in the ponds or reservoirs when disposed of into them. And this affects the aquatic life adversely. The samples were collected at 360 minutes intervals to estimate the COD. The reactors were operated until the COD was reduced to 250 mg/l (the Indian effluent discharge standards). COD is determined from Equation (1), which is reported in the literature [14].

$$\text{Chemical Oxygen Demand as mg O}_2\text{/L} = \frac{(A - B) \times M \times 8000}{\text{mL sample}} \tag{1}$$

where A is ml of ferrous ammonium sulphate used for the blank and B for the waste sample. M is the Molarity of the ferrous ammonium sulphate solution.

The wastewater degradation % is calculated from Eq. (2).

$$\% \text{ Degradation} = \frac{\text{COD}_{\text{Initial}} - \text{COD}_{\text{Final}}}{\text{COD}_{\text{Initial}}} \times 100 \tag{2}$$

The different hydrodynamic parameters obtained for the stirred tank reactor for the fixed operating condition of wastewater treatment are explained in the next section.

3. Parameters estimated

Following experiments (Table 2) were performed for the stirred tank reactor with a dual impeller.

Table 2. Set of effluent treatments performed for in stirred tank reactor with a dual impeller Ruston turbine.

Sr.No	Superficial gas velocity (m/s)	Speed of impeller RPM	Normalized impeller clearance (h/T) C1 Case	Normalized impeller clearance (h/T) C2 Case
1	0.00023	120	0.86	1.2
2		170	0.86	1.2
3		220	0.86	1.2
4		270	0.86	1.2
1	0.0007	120	0.86	1.2
2		170	0.86	1.2
3		220	0.86	1.2
4		270	0.86	1.2
1	0.0011	120	0.86	1.2
2		170	0.86	1.2
3		220	0.86	1.2
4		270	0.86	1.2
1	0.0016	120	0.86	1.2
2		170	0.86	1.2
3		220	0.86	1.2
4		270	0.86	1.2

3.1. Gas hold-up (ε_G)

The hold-up of gas is very important for the hydrodynamics of a packed bed or any gas liquid contactor. The transport and hydrodynamic behaviour of the combined phases depends on the holdup and gas velocity. Mass transfer and liquid circulation are affected by hold-up. They can be

determined for the reactor volume by using the equation below [23]:

$$\epsilon_G = \left[1 - \frac{\Delta P}{\Delta P_0} \right] \tag{3}$$

where ΔP is the dynamic pressure. It was measured by a pressure sensor in the stirred tank reactor at U_G > 0; ΔP₀ denotes the static pressure at U_G = 0.

3.2. Bubble size distribution (d_B)

For gas liquid mass transfer, when gas is bubbled in a continuous liquid phase, the formation of bubbles is an important phenomenon. As per the theories of mass transfer, the bubble formations and their collapse have an effect on microscopic mass transfer. The distribution of bubble size in the reactor and the number of bubbles vary with superficial gas velocity and impeller speed in the stirred tank reactor. Major axis 2a and minor axis 2b of the bubbles are utilized to determine the diameter (equivalent) of a bubble. The equivalent diameter, D_{eq} , is obtained from Eq. (4). The below-mentioned correlations are reported in the literature [24]. These can be used for determining the equivalent diameter

$$D_{eq} = 2\sqrt[3]{a^2b} \quad (4)$$

$$d_{bs} = \frac{\sum_i^N n_i d_{Bi}^3}{\sum_i^N n_i d_{Bi}^2} \quad (5)$$

where n_i is the number of the bubbles with individual diameter d_{Bi} ; this method has been described in the literature [25].

3.3. Specific power consumption

The power requirement needs to be optimum for the efficient performance of the equipment. The power delivered to the fluid is a function of angular velocity $2\pi N$ and torque τ . The following equation calculates the aerated power consumption [24].

$$P_G = 2\pi N \tau \quad (6)$$

where N and τ denote the speed of the impeller and the total torque acting on all blades, respectively. The values of torque were determined from simulations and experimentations. The total specific power is determined for both impeller configurations. Eq. 7 is proposed by the researcher [24].

$$\left(\frac{P_G}{V_L}\right)_{Total} = \left(\frac{P_G}{V_L}\right) + \rho_L g U_g \quad (7)$$

where $\left(\frac{P_G}{V_L}\right)$ can be determined from the torque on the blades. The quantity, $(\rho_L g U_g)$, was estimated from superficial gas velocity. The velocity introduced at the bottom of the reactor was considered for the same. Acceleration due to gravity is indicated by g , ρ_L is the density of the

working fluid. V_L is the total volume of the working fluid in the stirred tank reactor.

3.4. Volumetric mass transfer coefficient

The coefficient of volumetric mass transfer gives an idea about the extent of the mass transfer taking place between the two phases. The volumetric mass transfer coefficient ($k_L a$) was determined graphically for both reactors. The graphical method is described in the literature [23]. Nitrogen was added to reduce the concentration of oxygen to near zero. The coefficient of diffusivity for the diffusion of air into water was $D_L = 20.0 \times 10^{-8} \text{ m}^2/\text{s}$. The density of water was $998 \text{ kg}/\text{m}^3$. The value of surface tension was $0.072 \text{ N}/\text{m}$ and the dynamic viscosity was $0.000899 \text{ kg}/\text{ms}$. The experiment was performed at a temperature of 30°C . The equilibrium dissolved oxygen concentration of $7.5 \text{ mg}/\text{l}$ was used in Eq. (8). Varying operating conditions were tested, as shown in Table 3. Two dissolved oxygen probes were used in the stirred tank reactor. The data acquisition system was employed to record the dissolved oxygen concentration vs. time data for both probes. The value of oxygen concentration vs. time was recorded for both probes separately during an experiment. The average slope of concentration vs. time data of two probes was determined. The volumetric mass transfer coefficient was determined in the stirred tank graphically. The material balance for the dissolved oxygen in liquid could be established as

$$\frac{dc}{dt} = k_L a (c^* - c) \quad (8)$$

where c , dc/dt , and c^* are the oxygen concentration, concentration gradient of a liquid phase, and dissolved oxygen concentration at equilibrium, respectively. Some methods for measuring are incorporated with Eq. (8). The volumetric mass transfer coefficient is calculated from Equation 8. It is first integrated, and the graph of $\ln\left(\frac{c^* - c}{c^* - c_0}\right)$ vs. time is plotted.

$$\ln\left(\frac{c^* - c}{c^* - c_0}\right) = k_L a (t) \quad (9)$$

The mass transfer coupled to bubble size (d_B) depends on the interfacial area (a_i) and global gas hold-up (ϵ_G). The specific interfacial area is given by the following equation [25]:

$$a_i = \frac{6 \epsilon_G}{d_B (1 - \epsilon_G)} \quad (10)$$

The experimental volumetric mass transfer coefficient for the Rushton and curved blade turbine in the stirred tank reactor with different mass transfer models were compared with others in the literature [26]. Experimental values of the mass transfer coefficient for C1 and C2 cases in the stirred tank reactor were compared with values obtained from different models. The renewal rate of liquid was controlled by the bubble flow relative to the gas flow. The slip velocity model for the mass transfer coefficient prediction in the present study is given as follows:

U_{slip} is the slip velocity of the two phases (gas and liquid) and a_i is the specific interfacial area.

$$k_L^{\text{slip velocity}} a_i = \frac{6 \epsilon_G}{d_B (1 - \epsilon_G)} \times \frac{2}{\sqrt{\pi}} \sqrt{\frac{D_1 U_{\text{slip}}}{d_B}} \quad (11)$$

where U_{slip} is the slip velocity of the two phases (gas and liquid) and a_i is the specific interfacial area.

4. Mathematical modelling

4.1. Governing Equation

The hydrodynamics in the stirred tank reactor was simulated using the Eulerian approach in combination with the population balance model (PBM). The continuous and dispersed phases were considered as supported by interpenetrating media. The finite volume approach was used for solving the equations. The standard k-epsilon turbulent model was used to predict the different hydrodynamic parameters in the current simulation. The interfacial forces between the gas and liquid phase were incorporated in the present simulation, as shown in Table 3.

4.2. Population balance model for bubble size distributions

The population balance model is included in the present simulation. The bubble break-up phenomenon is incorporated into the simulation. The type of flow encountered in the stirred tank reactor is called polydisperse multiphase flow. A broad range of size groups are present in multiphase flow. In polydisperse multiphase flow, phases interact via various processes. A population balance is required to explain the flow. Population balance is a well-established method for

determining the size distribution of the dispersed phase. It also takes into account the breakage and coalescence effects in different sparger configurations. A general form of the population balance is Eq. (12).

$$\frac{\partial n_i}{\partial t} + \nabla \cdot (u_G n_i) = B_B + B_C - D_B - D_C \quad (12)$$

where u_G and n_i represent the gas velocity and the number density of size group i ; the terms B_B , B_C , D_B , and D_C are respectively the "birth" and "death" due to the break-up and coalescence of bubbles. The discrete method is used in the population balance model.

4.3. Grid Independence Study

The grid independence test was conducted independently by the stirred tank reactor for C1 and C2 cases. The computational grid and solution domain in a reactor is shown in Figure 2. The different grid sizes of the stirred tank reactor were configured by the dual impeller Rushton turbine, as shown in Table 4.

The four-grid size is considered in the stirred tank reactor for the dual impeller Rushton turbine for C1 and C2 cases. The overall gas hold-up and power consumption were determined in a stirred tank reactor at a superficial gas velocity of 0.0016 m/s and impeller speed of 270 rpm, as shown in Figure 3. It was observed that similar results of power consumption and overall gas hold-up using a grid size of 500300 (Grid-3) and 761388 (Grid-4). Hence, 500300 (Grid-3) was adapted for further simulation.

4.4. Bin Sensitivity Study

For the present simulation, a bin sensitivity study was conducted. The operating parameters were kept at 270 rpm, and the superficial gas velocity at $U_G = 5.76$ m/h. The number of bins varied, keeping the minimum and maximum value of bubble size constant. Four bin numbers selected were 7, 9, 12, and 23. The least bubble size was 0.1 mm, while the maximum bubble size was kept at 0.016.32 m. This minimum and maximum bubble size was predicted using the experimental data uniform distribution of bubble size. Different bins are discretized as follows in Eq. (13):

$$\frac{d_{i+1}}{d_i} = 2^q \tag{13}$$

where q = 3.66, 2.75, 2, 1 for bins 7, 9, 12, and 23, respectively. For the bin sensitivity study, three locations were selected with corresponding height

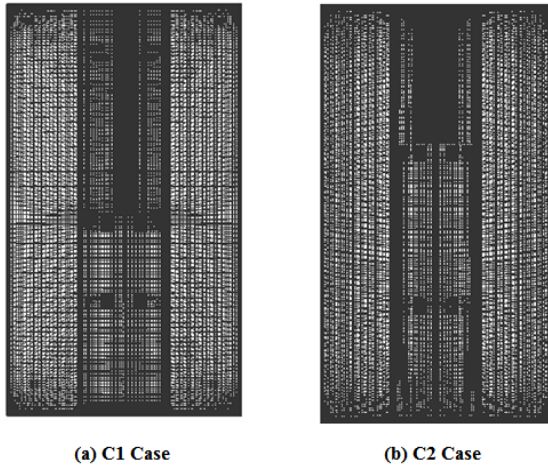
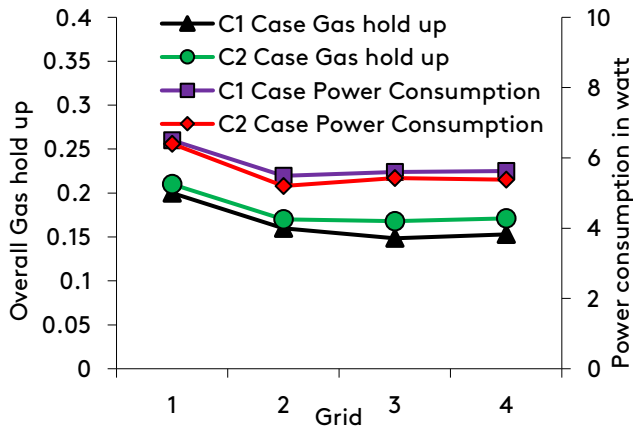
ratios as follows H/h = 3.4286, 2.353, and 1.348, respectively. Simulation results of different bins 7, 9, 12, and 23 of bubble size vs. % were plotted. It can be seen that the experimental bubble size vs. % data for bin 23 data was in good agreement. So, bin 23 was selected for further simulation.

Table 3. Governing Equations.

Sr.No	Equation Name	Equation Expression
1	Continuity	$\frac{\partial}{\partial t}(\rho_k \epsilon_k) + \nabla(\rho_k \epsilon_k u_k) = 0$
2	Momentum	$\sum_{k=1}^n \alpha_k = 1$ $\frac{\partial}{\partial t}(\rho_k \epsilon_k u_k) + \nabla(\rho_k \epsilon_k u_k u_k) = \nabla \tau_{effi} - \epsilon_k \nabla P + \epsilon_k \rho_k g + R_i + F_i$
3	Interfacial forces	$R_i = -R_g = E(U_G - U_L)$ Where E is the gas-liquid exchange coefficient given as: $E = \frac{3}{4} \rho_L \epsilon_L \epsilon_G \frac{C_D}{d_B} U_G - U_L $
4	Drag Force (M _{D,L})	$\frac{C_D - C_{Do}}{C_{Do}} = K \left(\frac{d_B}{\lambda}\right)^3$ $C_{Do} = \max\left\{\left(\frac{2.667E_o}{E_o + 4.0}\right), \left(\frac{24}{Re_B} (1 + 0.15Re_B^{0.687})\right)\right\}$ Where K = 6.5 × 10 ⁻⁶ is used in the present equation. Many researchers have recommended the above correlation in literature [27,28]
5	The lift coefficient (M _{L,L})	$M_{L,L} = -C_L \rho_L \alpha_G (u_G - u_L) \times (\nabla \times u_L)$ $C_L = \begin{cases} \min[0.288 \tanh(0.121Re), f(E_{od})] & E_{od} < 4 \\ f(E_{od}) = 0.00105E_o^3 - 0.0159E_{od}^2 - 0.0204E_{od} + 0.474 & 4 \leq E_{od} \leq 10 \\ -0.29 & E_{od} > 10 \end{cases}$ The above correlation has been suggested in the literature [29]
6	Virtual mass force (M _{VM,L})	The virtual mass force's effect is insignificant in the bulk region of stirred vessels.
7	Turbulent Dispersion Force (M _{TD,L})	$M_{TD,L} = C_{TD} \rho_L K \nabla \alpha_g$ Where C _{TD} = 0.2 The values were suggested by literature [30]
8	Wall Lubricating Force (M _{WL})	$M_{WL} = \frac{-\alpha_G \rho_L (U_G - U_L)}{D_S} \max\left(0, C_{W1} + C_{W2} \frac{D_S}{y_w}\right) n_w$
9	Turbulent kinetic energy (k)	$\frac{\partial}{\partial t}(\rho_L \epsilon_L k_L) + \nabla \frac{\partial}{\partial t}(\rho_L \epsilon_L \epsilon) + \nabla(\rho_L \epsilon_L u_L \epsilon)$ $= \nabla \cdot \left(\epsilon_L \frac{\mu_{eff,L}}{\sigma_\epsilon} \nabla \epsilon_L\right) - \epsilon_L \frac{\epsilon}{K} (C_{\epsilon 1} G_{kL} - C_{\epsilon 2} \rho_L \epsilon) + \rho_L \epsilon_L \Pi_{\epsilon L}$
	Turbulent dissipation rate (ε)	Constant values C _{ε1} = 1.44, C _{ε2} = 1.92, σ _k = 1.0 and σ _ε = 1.3 $(\rho_L \epsilon_L u_L k_L) = \nabla \cdot \left(\epsilon_L \frac{\mu_{eff,L}}{\sigma_k} \nabla k_L\right) - \epsilon_L (G_{kL} - \rho_L \epsilon_L) + \rho_L \epsilon_L \Pi_{kL}$

Table 4. Different grid sizes for stirred tank reactor.

Sr. No	Grid	Stirred tank reactor with dual impeller elements
1	1	300500
2	2	400100
3	3	500300
4	4	761388

**Fig. 2.** Computational grid and solution domain of the stirred tank reactor with dual impeller Rushton turbine.**Fig. 3.** Simulation results with different grids ($N = 270$ rpm, $U_G = 0.0016$ m/s) for impeller configuration C1 and C2 case for the effect of a grid on power consumption and overall gas hold-up.

4.5. Numerical solution

CFD simulations were performed using ANSYS Fluent software. The following Eq. (14) is reported in the literature [31] for the size of bubbles generated at the sparger. The sparger had 32 openings; each hole on the sparger became 3 mm in diameter.

$$d_b = \left(\frac{6 \sigma d_s}{g (\rho_l - \rho_g)} \right)^{1/3} \quad (14)$$

The calculated diameter of $d_b = 5.1$ mm; thus, the size fraction of the 6th bubble group with a diameter of 5.0 mm was set to be unity for the inlet condition. In all simulations, air with a density and viscosity of 1.225 g/l and 17.894×10^{-6} kg/ms, respectively, was used as a dispersed phase. Water with a density and viscosity of 998.2 kg/m³ and 10.03×10^{-4} kg/ms, respectively, was used as a continuous phase. The convergence criterion for all transport equations was set as 0.1×10^{-4} .

5. Results and discussion

5.1. Effect of superficial gas velocity on the % degradation of wastewater for both impeller configurations.

The superficial gas velocity was an important parameter in the process of degradation of wastewater. Initially, only superficial air velocity was used in the range of 0.828 m/h to 5.76 m/h. It was observed that at low superficial air velocity, 60.8% degradation was achieved, which increased to 65.8 % at 0.00070 m/s and then to 70.12 % at 0.0011 m/s. The increase in COD reduction rate was due to a gas hold-up, which was directly proportional to the impeller speed and superficial air velocity, improving the mass transfer rate. With a further increase in superficial air velocity to 0.0016 m/s, the % degradation decreased to 67.18%, less than achieved at 0.0011 m/s. It might be due to a higher superficial gas velocity and turbulent flow in the reactor, which resulted in the fluid dynamic effect that increased the shear stress on immobilized microbial cells. Eddies are smaller than the microbial cells, interact more powerfully with them and generate shearing. The influence of eddy size on the shearing of cells has been reported in the literature [32]. According to the literature [33], the threshold of tolerance to shear stresses is not known in the range from 0 to 80 Pa. The above threshold value of shear stress-induced is decreased in the microorganism viability. Hence, this effectively decreases the % degradation. A COD reduction of 70.12 % was obtained at an optimized superficial gas velocity value of 0.0011 m/s after 32 hr, as shown in Figure 4. Thus, a superficial gas velocity of 0.0011 m/s could be considered adequate for the survival of microorganisms.

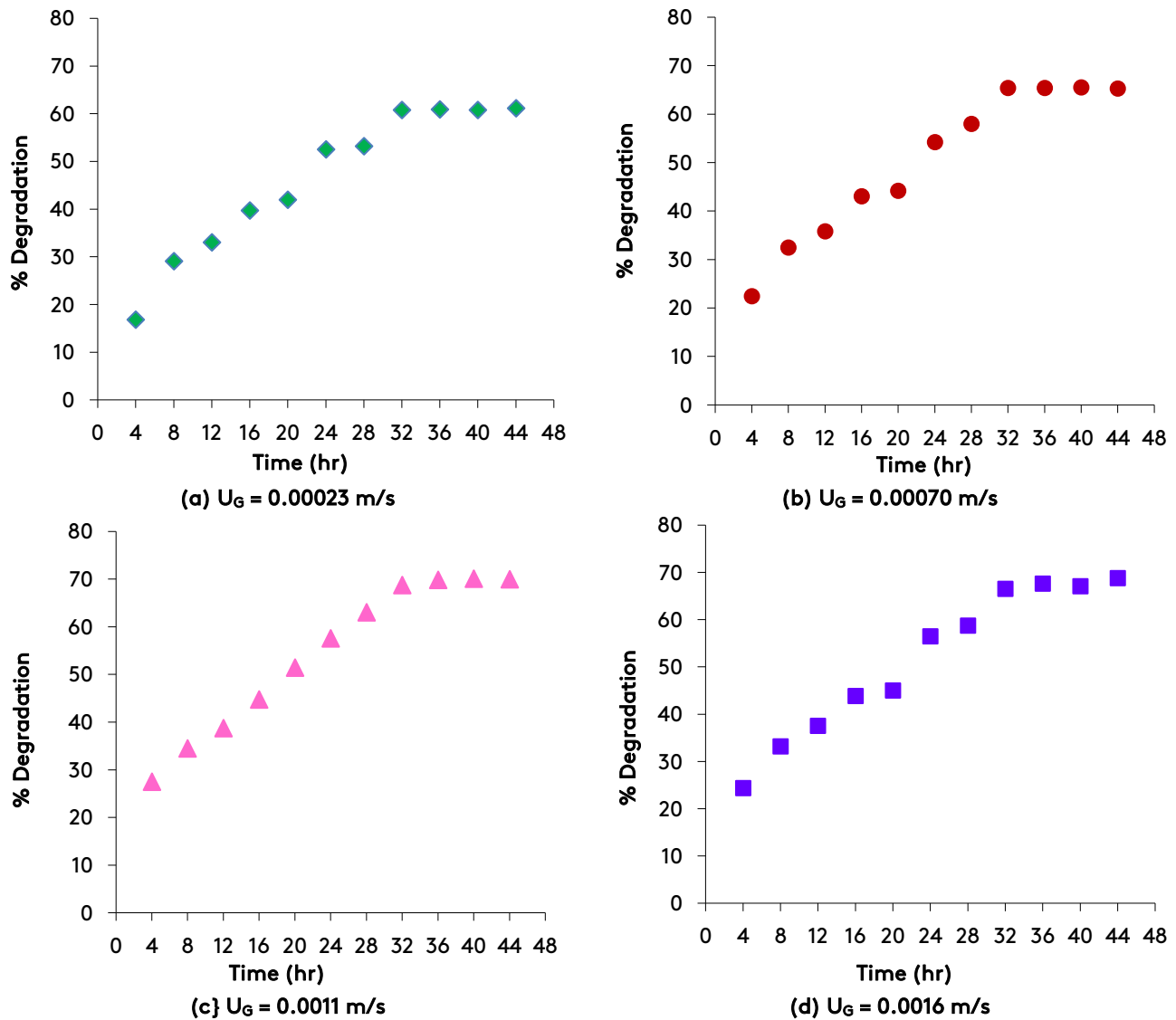


Fig. 4. Comparison of % degradation vs. time for different superficial gas velocity.

5.2. Effect of impeller speed on the % degradation of wastewater for both impeller configurations.

The experiments were conducted at impeller speeds from 120 to 270 rpm at an optimized value of superficial gas velocity, i.e., 0.0011 m/s for both C1 and C2 impeller configurations. At the impeller speed of 120 rpm, 71.32 % degradation was observed for the C1 impeller and 78.21% for the C2 configuration after 36 hr. The C2 impeller configuration gave a better degradation % under identical operating conditions. It was also observed that with an increase in rotation speed up to 170 rpm, COD removal increased significantly for both the C1 and C2 impeller configurations, as shown in Figures. 5 and 6. Further experiments were conducted for impeller speeds of 170 and 270 rpm

for both impeller configurations. From Figure 6, it can be seen that for an impeller speed at 170 rpm, 80.8% degradation was obtained for the C2 impeller configuration after 36 hr. For the C1 impeller configuration, 74.21% of degradation was obtained, as shown in Figure 5. No significant increase in COD removal was observed by increasing rotation speed beyond 170 rpm for the C1 and C2 impeller configurations. This may be due to the effect of fluid dynamics and complete mixing. The experiments were conducted for both impeller configurations in the stirred tank reactor for similar operating conditions. From the experimental results, a volumetric mass transfer coefficient equal to 0.12 1/s was obtained for the C1 case and 0.14 1/s for the C2 case at an optimized superficial

gas velocity ($U_G = 0.0011\text{m/s}$) and an impeller speed of 170 rpm. It was observed that the power consumption was lesser by 1.75 watts for the C1 impeller configuration than the C2 impeller configuration (1.8 watts) under optimized superficial gas velocity. The hydrodynamic parameters were estimated in the stirred tank reactor for an optimized superficial gas velocity of 0.0011 m/s, as shown in Table 5.

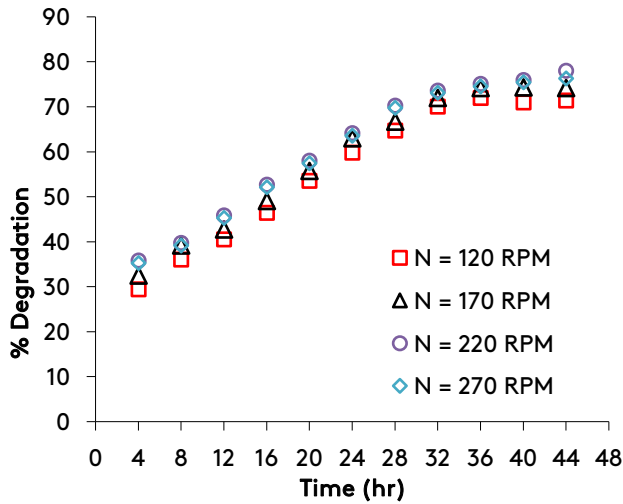


Fig. 5. % Degradation vs. time for impeller configuration of C1 Case for optimized superficial gas velocity $U_G = 0.0011\text{m/s}$.

Table 5. The comparison of experimental values of stirred tank reactor for optimized superficial gas velocity for the cases of C1 and C2.

Reactor Configuration	Optimized superficial gas velocity (U_G) m/s	Impeller speed rpm	Power consumption (P) watt	Total specific power consumption (P_G/V_L) W/m^3	Sauter mean bubble diameter d_s (m)	Specific Interfacial area (a) m^2/m^3	Mass Transfer coefficient ($K_L a \times 10^3$) (1/s)
Stirrer Tank Reactor C1 Case	0.0011	120	0.72	32	0.00281	91.98	0.39
		170	1.75	60	0.00246	140.04	0.47
		220	3.1	98	0.0021	258.60	0.52
		270	5.19	156	0.00132	679.20	0.60
Stirrer Tank Reactor C2 Case	0.0011	120	0.79	33	0.00225	183.86	0.45
		170	1.8	64	0.00152	420.16	0.54
		220	3.21	101	0.00126	667.86	0.62
		270	5.67	169	0.00115	942.46	0.69

The pressure measuring techniques described previously in section 4 were used for the measurement of the hold-up of gas. For the impeller configuration, the C1 and C2 case gas hold-up was compared for the superficial gas velocity from 0.00023 to 0.0016 m/s for the impeller speed of 120 to 270 rpm. Gas hold-up plays an essential role in mass transfer for aerobic wastewater treatment. In the wastewater treatment process, oxygen is essential for the

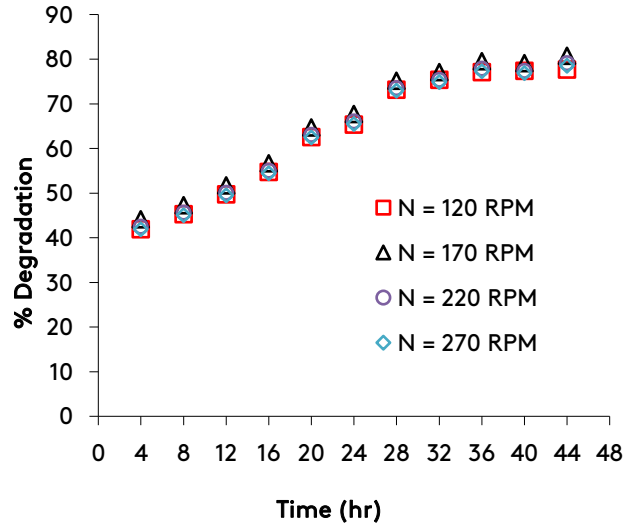
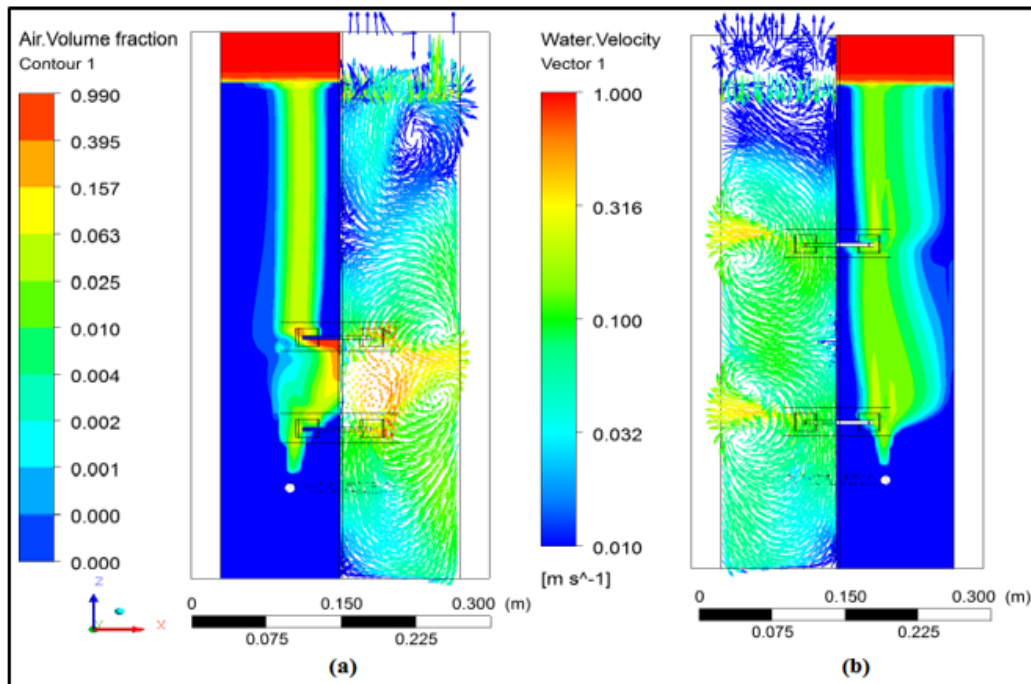


Fig. 6. % Degradation vs. time for impeller configuration for C2 Case for optimized superficial gas velocity $U_G = 0.0011\text{m/s}$.

microorganisms to stay alive. The gas hold-up generally increases with superficial gas velocity. The effect of bubble interaction within the reactor depends on wastewater properties. In the biological wastewater treatment process, the property of wastewater changes due to the microorganism degradation of wastewater and the generation of microbes. For higher operating conditions, wastewater treatment in a stirred tank reactor is complicated. Aerobic microbes are highly

shear sensitive and stand in harsh, turbulent flow conditions. For the present work, superficial gas velocity and impeller speed were optimized to ensure that shear-sensitive aerobic microorganisms were growing properly. Also, it was needed to ensure that there was adequate mass transfer and minimum cell damage. For this operating condition, the flow regime had become a limited gas recirculation regime corresponding to vortex clinging (VC). From the CFD simulation, it can be found that capturing the limited gas recirculation regime corresponded to vortex clinging (VC) for the optimized superficial gas velocity of 0.00118 m/s and impeller speed of 170 to 220 rpm for the C1 & C2 impeller configuration. The CFD simulation in comparison of the combined contour and vector of air volume fraction and liquid circulation velocity for the cases of C1 and C2 is as shown in Figure 7 (a and b). Thus, a lower impeller speed (170 rpm) gave a better gas hold-up and liquid circulation was observed in the C2 case compared to the C1 case, as shown in Figure 7 (a

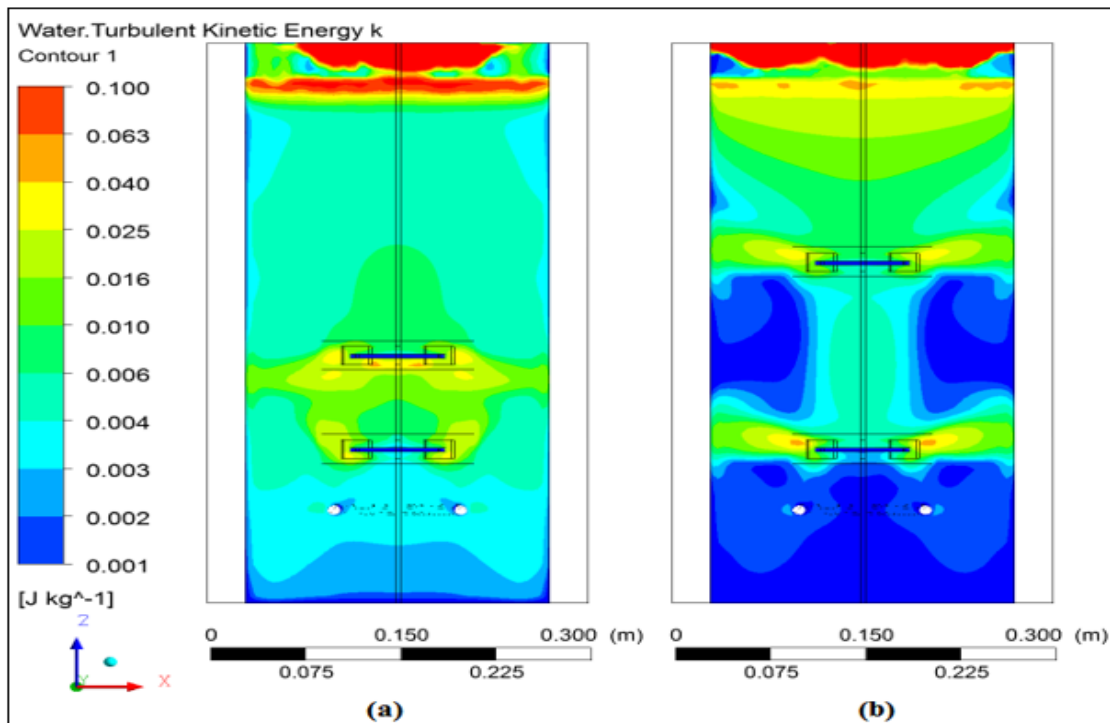
and b). The power consumption generally depends on the impeller's type, speed, and apparent viscosity of the medium. For the C1 case, both impellers were nearer to each other and acted as a single impeller. When clearance between the impellers increased, both impellers acted as individual impellers. The significantly affected flow pattern by the clearance between the impellers for the dual Rushton turbine in the stirred tank reactor has been reported in the literature [34]. For the present work, the impeller speed was 170 rpm, and the power consumption for the C2 case was higher (1.8 watt) than for the C1 case (1.75 watt) to optimize the superficial gas velocity. CFD simulation can capture turbulent kinetic energy and dissipation rate for optimized conditions, as shown in Figures. 8 and 9 (a and b). The combination of air volume fraction and water velocity vector for three axial locations ($Z = 165$ mm, $Z = 265$ mm, and $Z = 365$ mm) in the stirred tank reactor was captured, as shown in Figure 10 (a and b).



W.r.t. the vertical plane stirred tank reactor for impeller configuration for optimized superficial gas velocity

0.0011 m/s (a) C1 case $N = 220$ rpm (b) C2 case $N = 170$ rpm.

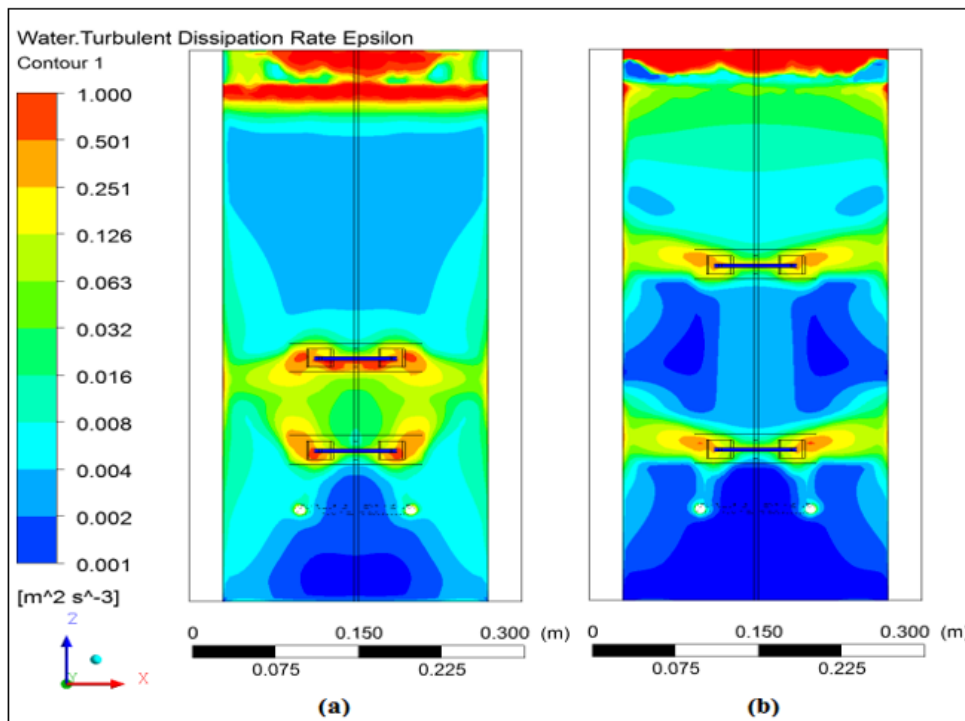
Fig. 7. Combined contour and vector of air volume fraction and water velocity.



C1 & C2 impeller configuration for optimized superficial gas velocity 0.0011 m/s

(a) C1 case N = 220 rpm (b) C2 case N = 170 rpm.

Fig. 8. Comparison of water turbulent kinetic energy on the vertical plane in stirred tank reactor.



C1 & C2 impeller configuration for optimized superficial gas velocity 0.0011 m/s (a) C1 case N = 220 rpm (b)

C2 case N = 170 rpm.

Fig. 9. Comparison of water turbulent dissipation rate on the vertical plane in stirred tank reactor.

In the present work, the gas hold-up for the C1 and C2 cases was compared for superficial gas velocity from 0.00023 to 0.0016 m/s with an impeller speed from 120 to 270 rpm. Figure 11 shows the effect of gas hold-up on specific power consumption compared to the optimized superficial gas velocity (0.00118 meter per second) and the impeller speed of 120 to 270 rpm for the C1 and C2 impeller cases. The gas hold-up obtained from the experimental and the predicted CFD simulation was in excellent sync, as shown in Figure 11. In the stirred tank reactor without impeller speed, 70% degradation was achieved for a superficial gas velocity of 0.0011 m/s. This optimized superficial gas velocity was further used for wastewater treatment in the stirred tank reactor for different impeller speeds

and configurations of the C1 and C2 cases. For the C1 impeller case, a 74.21% extent of degradation was achieved for an impeller speed of 170 rpm. Thus, for the same operating condition for the C2 case, 80.8% degradation was achieved for the wastewater in the stirred tank reactor. The stirring favoured the growth and performance of these microorganisms in the STR bioreactor. For higher superficial gas velocity and impeller speed, the problem of shearing also occurred. The gas hold-up vs. power consumption with the experimental and CFD validations were in good agreement. Fig. 12 and Table 6 depict the experimental and predicted mass transfer coefficients and the comparison from different models with impeller speed for optimization.

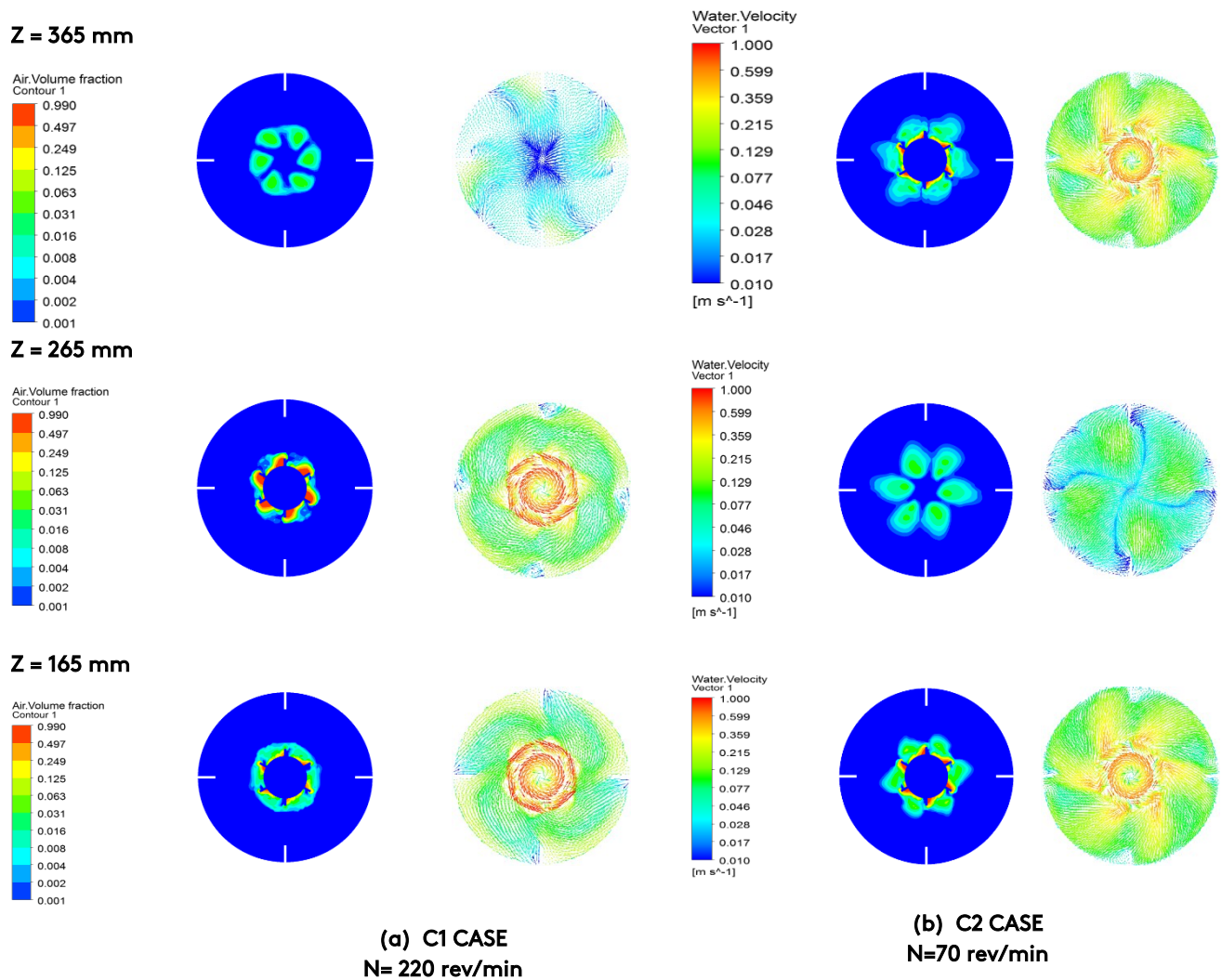
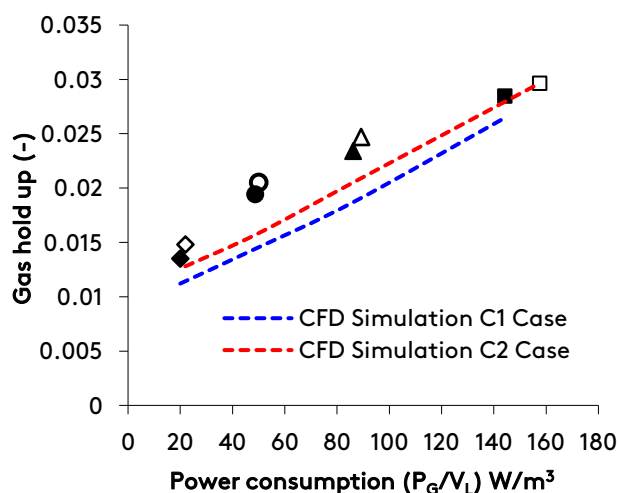


Fig. 10. Combination of air volume fraction and water velocity vector for different axial locations C1 and C2 case for $U_G = 0.00118$ m/s.

Table 6. Comparison of different mass transfer coefficient models with experimental for impeller configuration C1 and C2 cases at different impeller speeds.

Reactor Configuration	Optimized Superficial gas velocity (U_G) m/s	Impeller speed in rpm	$K_L a \times 10^3$ (1/s) CFD Simulation				Experimental $K_L a \times 10^3$ (1/s)
			Penetration model	Eddy cell model	Slip velocity model	Rigid cell model	
Stirrer Tank Reactor C1 Case	0.00118	120	0.8	0.05	0.46	0.09	0.39
		170	0.85	0.054	0.51	0.098	0.47
		220	0.9	0.056	0.56	0.11	0.52
		270	0.93	0.058	0.61	0.13	0.6
Stirrer Tank Reactor C2 Case	0.00118	120	0.9	0.059	0.5	0.12	0.45
		170	0.92	0.061	0.57	0.13	0.54
		220	0.95	0.063	0.63	0.15	0.62
		270	0.98	0.068	0.69	0.17	0.69

**Fig. 11.** Comparison between experimental and CFD simulation results C1 and C2 impeller configuration over different impeller speed (1) 120 rpm C1 (◆) C2 (◇) (2) 170 rpm C1 (●) C2 (○) (3) 220 rpm C1 (▲) C2 (△) (4) 270 rpm C1 (■) C2 (□) (5) CFD Simulation C1 Case (---) (6) CFD Simulation C2 Case (---) for optimized superficial gas velocity $U_G = 0.00118$ m/s.

The homogenous discrete method was adopted to accurately predict the bubble size distribution in the stirred tank reactors. The air means bubble diameter was compared to that predicted from the CFD-PBM simulation of the optimized superficial gas velocity of 0.0011 m/s for the C1 and C2 cases, as shown in Figure 13. The different mass transfer models include the penetration, slip velocity, rigid cell, and eddy cell models, which were compared for an impeller speed of 120 to 270 rpm for the optimized superficial gas velocity of 0.00118 m/s. It can be seen from Figures 12 (a) and (b) that the slip velocity model gave a better volumetric mass transfer coefficient prediction for the C1 and C2 cases. Further simulation of the slip velocity model was used to estimate the mass transfer in the reactor. Figure 14 depicts the mass transfer coefficient for the slip velocity model from the CFD contour.

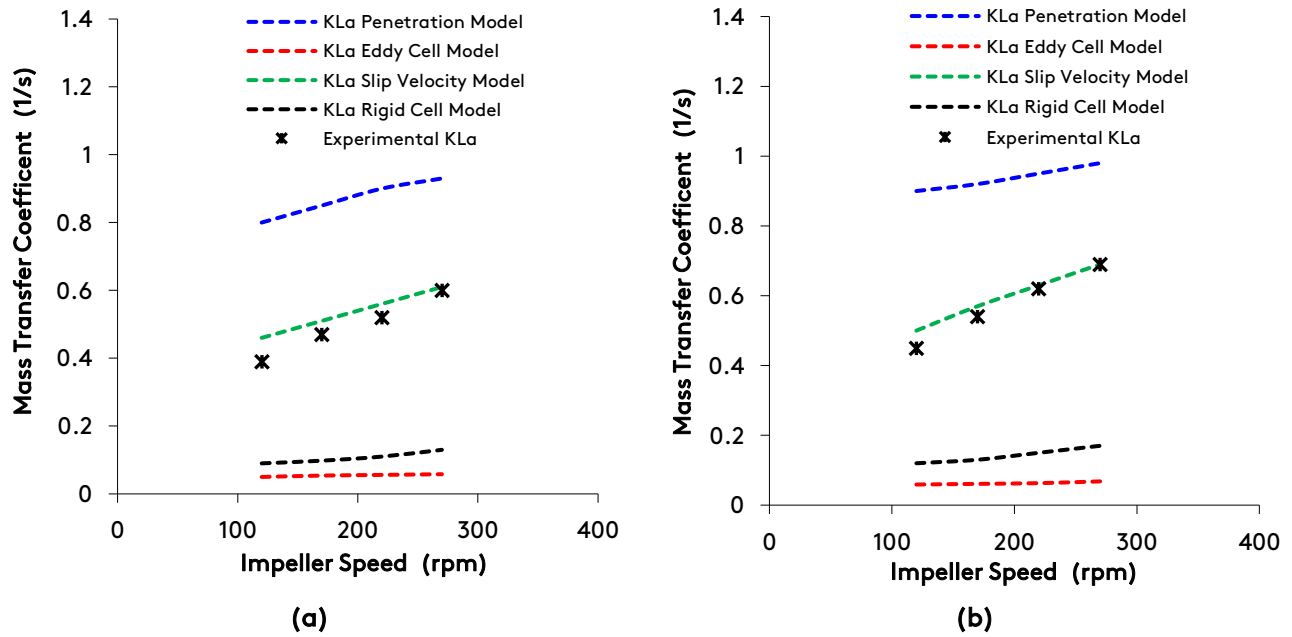
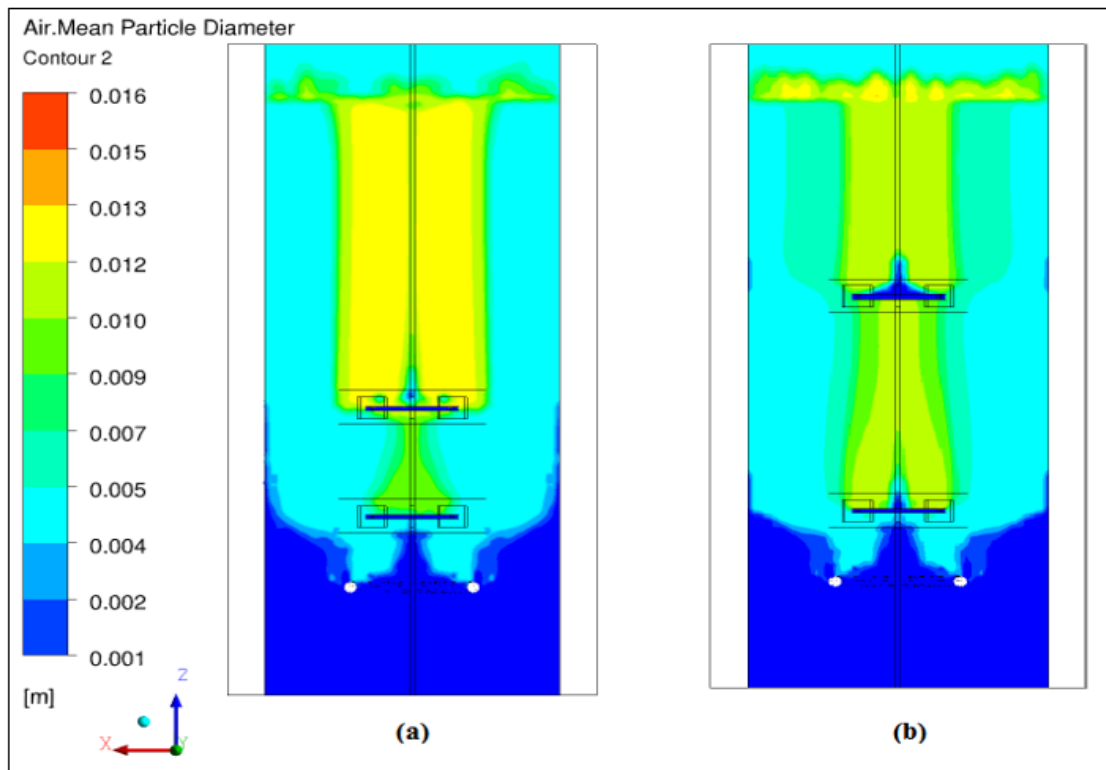
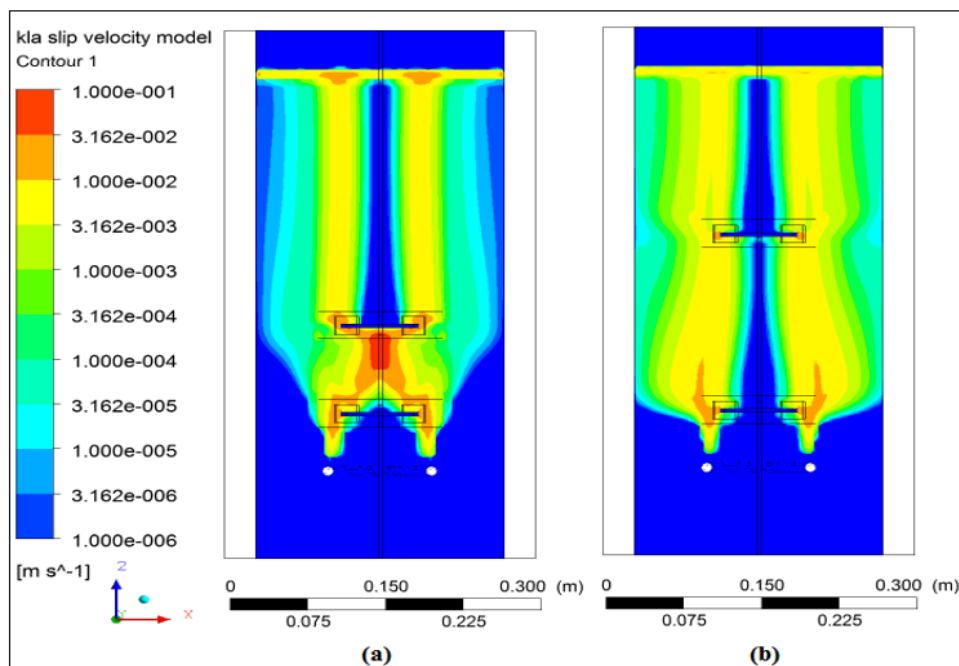


Fig. 12. Experimental and predicted of volumetric mass transfer coefficients from different models impeller speed for optimized $U_G = 0.00118$ m/s (a) C1 case (b) C2 case.



C1 and C2 cases for optimized superficial gas velocity 0.00118 m/s (a) $N = 220$ rpm (b) $N = 170$ rpm
 Fig. 13. Comparison of predicted air mean bubble diameter.



C1 and C2 cases for optimized superficial gas velocity 0.0011 m/s (a) $N = 220$ rpm (b) $N = 170$ rpm

Fig. 14. Comparison of predicted volumetric mass transfer coefficient.

6. Conclusions

Biological methods for the reduction of pollutants from liquid effluent can be optimized by using suitable techniques. The experimental results indicated that the percentage degradation increased with an increase in superficial velocity. Very high superficial velocity had a negative effect on the degradation. The degradation increased with impeller speed for an initial certain speed, and a further increase in the speed had an insignificant effect. CFD simulation was helpful for a complete detailed understanding of the hydrodynamics in the stirred tank reactors for the C1 and C2 cases. The hydrodynamic parameters were compared with CFD simulation. The results were found to confirm each other's values, practical and theoretical. In a comparison of the C1 case and C2 case for the same 170 rpm speed, 80.8% degradation wastewater was obtained for the C2 case. The results also indicated more degradation in the C2 case. The slip velocity model gave a better mass transfer coefficient prediction among all the mass transfer models. The model based on the fluid dynamics software tools and theory of population balance could be used for designing and developing reactors for liquid effluent treatment on an industrial scale. This enabled the authors to explore

more options in terms of contact patterns and contact equipment. It could be concluded that wastewater treatment methods like the activated sludge process and aeration could be carried out in a stirred tank reactor more effectively with detailed analysis of the flow patterns, impeller speed and position, velocity, and their effect on degradation. Modern simulation tools can save on resources considerably, making the technology more acceptable and economical.

Acknowledgments

We would like to thank the affiliating institute (GIT) for providing the funding for the design of the lab-scale reactors.

References

- [1] Gogate, P. R., Pandit, A. B. (2004). A review of imperative technologies for wastewater treatment I: oxidation technologies at ambient conditions. *Advances in Environmental Research*, 8(3-4), 501-551. [https://doi.org/10.1016/S1093-0191\(03\)00032-7](https://doi.org/10.1016/S1093-0191(03)00032-7)
- [2] Pittoors, E., Guo, Y., Van Hulle, S. W. (2014). Oxygen transfer model development based on activated sludge and clean water in diffused aerated cylindrical tanks. *Chemical Engineering Journal*, 243, 51-59.

- <https://doi.org/10.1016/j.cej.2013.12.069>
- [3] Moussavi, G., Naddafi, K., Mesdaghinia, A., Deshusses, M. A. (2007). The removal of H₂S from process air by diffusion into activated sludge. *Environmental Technology*, 28(9), 987-993.
<https://doi.org/10.1080/09593332808618856>
- [4] Nadayil, J., Mohan, D., Dileep, K., Rose, M., Parambi, R. R. P. (2015). A study on effect of aeration on domestic wastewater. *International Journal of Interdisciplinary Research and Innovations*, 3(2), 10-15.
- [5] Fuchs, W., Binder, H., Mavrias, G., Braun, R. (2003). Anaerobic treatment of wastewater with high organic content using a stirred tank reactor coupled with a membrane filtration unit. *Water Research*, 37(4), 902-908.
[https://doi.org/10.1016/S0043-1354\(02\)00246-4](https://doi.org/10.1016/S0043-1354(02)00246-4)
- [6] Walker, G. M., Weatherly, L. R. (1999). Biological activated carbon treatment of industrial wastewater in stirred tank reactors. *Chemical Engineering Journal*, 75(3), 201-206.
[https://doi.org/10.1016/S1385-8947\(99\)00109-6](https://doi.org/10.1016/S1385-8947(99)00109-6)
- [7] Siddique, N. I., Munaim, M. S. A., Wahid, Z. A. (2015). Role of biogas recirculation in enhancing petrochemical wastewater treatment efficiency of continuous stirred tank reactor. *Journal of Cleaner Production*, 91, 229-234.
<https://doi.org/10.1016/j.jclepro.2014.12.036>
- [8] Esteves, B. M., Rodrigues, C. S., Boaventura, R. A., Maldonado-Hódar, F. J., Madeira, L. M. (2016). Coupling of acrylic dyeing wastewater treatment by heterogeneous Fenton oxidation in a continuous stirred tank reactor with biological degradation in a sequential batch reactor. *Journal of Environmental Management*, 166, 193-203.
<https://doi.org/10.1016/j.jenvman.2015.10.008>
- [9] Gargouri, B., Karray, F., Mhiri, N., Aloui, F., Sayadi, S. (2011). Application of a continuously stirred tank bioreactor (CSTR) for bioremediation of hydrocarbon-rich industrial wastewater effluents. *Journal of Hazardous Materials*, 189(1-2), 427-434.
<https://doi.org/10.1016/j.jhazmat.2011.02.057>
- [10] Kanaujiya, D. K., Pakshirajan, K. (2022). Mass balance and kinetics of biodegradation of endocrine disrupting phthalates by *Cellulosimicrobium funkei* in a continuous stirred tank reactor system. *Bioresource Technology*, 344, 126172.
<https://doi.org/10.1016/j.biortech.2021.126172>
- [11] Shen, R., Jing, Y., Feng, J., Zhao, H., Yao, Z., Yu, J., Chen, J., Chen, R. (2021) Simultaneous carbon dioxide reduction and enhancement of methane production in biogas via anaerobic digestion of cornstalk in continuous stirred-tank reactors: The influences of biochar, environmental parameters, and microorganisms. *Bioresource Technology*, 319, 124146.
<https://doi.org/10.1016/j.biortech.2020.124146>
- [12] Yadav M., Vivekanand, V. (2021). Combined fungal and bacterial pretreatment of wheat and pearl millet straw for biogas production – A study from batch to continuous stirred tank reactors. *Bioresource Technology*, 321, 124523.
<https://doi.org/10.1016/j.biortech.2020.124523>
- [13] Azimi, B., Abdollahzadeh-Sharghi, E., Bonakdarpour, B. (2021). Anaerobic-aerobic processes for the treatment of textile dyeing wastewater containing three commercial reactive azo dyes: Effect of number of stages and bioreactor type. *Chinese Journal of Chemical Engineering*, 39, 228-239.
<https://doi.org/10.1016/j.cjche.2020.10.006>
- [14] Ayare, S.D., Gogate, P.R. (2019). Sonocatalytic treatment of phosphonate containing industrial wastewater intensified using combined oxidation approaches. *Ultrasonics Sonochemistry*, 51, 69-76.
<https://doi.org/10.1016/j.ultsonch.2018.10.018>
- [15] Jawale, R. H., Gogate, P. R., Pandit, A. B. (2014). Treatment of cyanide containing wastewater using cavitation-based approach. *Ultrasonics Sonochemistry*, 21(4), 1392-1399.
<https://doi.org/10.1016/j.ultsonch.2014.01.025>
- [16] Samstag, R.W., Wicklein, E.A. (2014). A protocol for optimization of activated sludge mixing. *87th Annual Water Environment Federation Technical Exhibition and Conference. WEFTEC 2014*, 7, 3614-3640.
- [17] Do-Quang, Z., Cockx, A., Liné, A., Roustan, M. (1998). Computational fluid dynamics applied to water and wastewater treatment facility modeling. *Environmental Engineering and Policy*, 1, 137-147.
<https://doi.org/10.1007/s100220050015>

- [18] Amini, E., Mehrnia, M. R., Mousavi, S. M., Mostoufi, N. (2013). Experimental study and computational fluid dynamics simulation of a full-scale membrane bioreactor for municipal wastewater treatment application. *Industrial and Engineering Chemistry Research*, 52(29), 9930-9939.
<https://doi.org/10.1021/ie400632y>
- [19] Samstag, R. W., Ducoste, J. J., Griborio, A., Nopens, I., Batstone, D. J., Wicks, J. D., Laurent, J. (2016). CFD for wastewater treatment: an overview. *Water Science and Technology*, 74(3), 549-563.
<https://doi.org/10.2166/wst.2016.249>
- [20] Matko, T., Chew, J., Wenk, J., Change, J., Hofman, J. (2021). Computational fluid dynamics simulation of two-phase flow and dissolved oxygen in a wastewater treatment oxidation ditch. *Process Safety and Environmental Protection*, 145, 340-353.
<https://doi.org/10.1016/j.psep.2020.08.017>
- [21] Le Moullec, Y., Gentric, C., Potier, O., Leclerc, J. P. (2010). Comparison of systemic, compartmental and CFD modelling approaches: application to the simulation of a biological reactor of wastewater treatment. *Chemical Engineering Science*, 65(1), 343-350.
<https://doi.org/10.1016/j.ces.2009.06.035>
- [22] Joshi, J. B. (2001). Computational flow modelling and design of bubble column reactors. *Chemical Engineering Science*, 56(21-22), 5893-5933.
[https://doi.org/10.1016/S0009-2509\(01\)00273-1](https://doi.org/10.1016/S0009-2509(01)00273-1)
- [23] Teli, S. M., Pawar, V. S., Mathpati, C. (2020). Experimental and computational studies of aerated stirred tank with dual impeller. *International Journal of Chemical Reactor Engineering*, 18(3), 20190172.
<https://doi.org/10.1515/ijcre-2019-0172>
- [24] Bouaifi, M., Hebrard, G., Bastoul, D., Roustan, M. (2001). A comparative study of gas hold-up, bubble size, interfacial area and mass transfer coefficients in stirred gas-liquid reactors and bubble columns. *Chemical Engineering and Processing: Process Intensification*, 40(2), 97-111.
[https://doi.org/10.1016/S0255-2701\(00\)00129-X](https://doi.org/10.1016/S0255-2701(00)00129-X)
- [25] Bouaifi, M., Roustan, M. (1998). Bubble size and mass transfer coefficients in dual-impeller agitated reactors. *The Canadian Journal of Chemical Engineering*, 76(3), 390-397.
<https://doi.org/10.1002/cjce.5450760307>
- [26] Devi, T. T., Kumar, B. (2017). Mass transfer and power characteristics of stirred tank with Rushton and curved blade impeller. *Engineering Science and Technology, an International Journal*, 20(2), 730-737.
<https://doi.org/10.1016/j.jestch.2016.11.005>
- [27] Komori, S., Murakami, Y. (1988). Turbulent mixing in baffled stirred tanks with vertical-blade impellers. *AIChE Journal*, 34(6), 932-937.
<https://doi.org/10.1205/02638760152721613>
- [28] Rutherford, K., Lee, K. C., Mahmoudi, S. M. S., Yianneskis, M. (1996). Hydrodynamic characteristics of dual Rushton impeller stirred vessels. *AIChE Journal*, 42(2), 332-346.
<https://doi.org/10.1002/aic.690420204>
- [29] Tomiyama, A., Celata, G. P., Hosokawa, S., Yoshida, S. (2002). Terminal velocity of single bubbles in surface tension force dominant regime. *International Journal of Multiphase Flow*, 28(9), 1497-1519.
[https://doi.org/10.1016/S0301-9322\(02\)00032-0](https://doi.org/10.1016/S0301-9322(02)00032-0)
- [30] Roy, S. & Joshi, J. (2008). CFD Study of Mixing Characteristics of Bubble Column and External Loop Airlift Reactor. *Asia-Pacific Journal of Chemical Engineering*, 3, 97-105.
[https://doi.org/10.1016/S0301-9322\(02\)00032-0](https://doi.org/10.1016/S0301-9322(02)00032-0)
- [31] Miller, D. N. (1974). Scale-up of agitated vessels gas-liquid mass transfer. *AIChE Journal*, 20(3), 445-453.
<https://doi.org/10.1002/aic.690200303>
- [32] Buffo, M. M., Corrêa, L. J., Esperança, M. N., Cruz, A. J. G., Farinas, C. S., Badino, A. C. (2016). Influence of dual-impeller type and configuration on oxygen transfer, power consumption, and shear rate in a stirred tank bioreactor. *Biochemical Engineering Journal*, 114, 130-139.
<https://doi.org/10.1016/j.bej.2016.07.003>
- [33] Lange, H., Taillandier, P., Riba, J. P. (2001). Effect of high shear stress on microbial viability. *Journal of Chemical Technology and Biotechnology: International Research in Process, Environmental and Clean Technology*, 76(5), 501-505.
<https://doi.org/10.1002/jctb.401>

- [34] You, S. T., Raman, A. A. A., Shah, R. S. S. R. E., Mohamad Nor, M. I. (2014). Multiple-impeller stirred vessel studies. *Reviews in Chemical Engineering*, 30(3), 323-336.
<https://doi.org/10.1515/revce-2013-0028>